Electronic Supplementary Material (ESI) for Nanoscale.

Supplementary Information for:

Controllable and reversible DNA translocation through a single-layer molybdenum disulfide nanopore

Wei Si*, Yin Zhang, Jingjie Sha, Yunfei Chen*

Jiangsu Key Laboratory for Design and Manufacture of Micro-Nano Biomedical Instruments, School of Mechanical Engineering, Southeast University, Nanjing, 210096, China

*The correspondence should be addressed to yunfeichen@seu.edu.cn, wei.si@seu.edu.cn

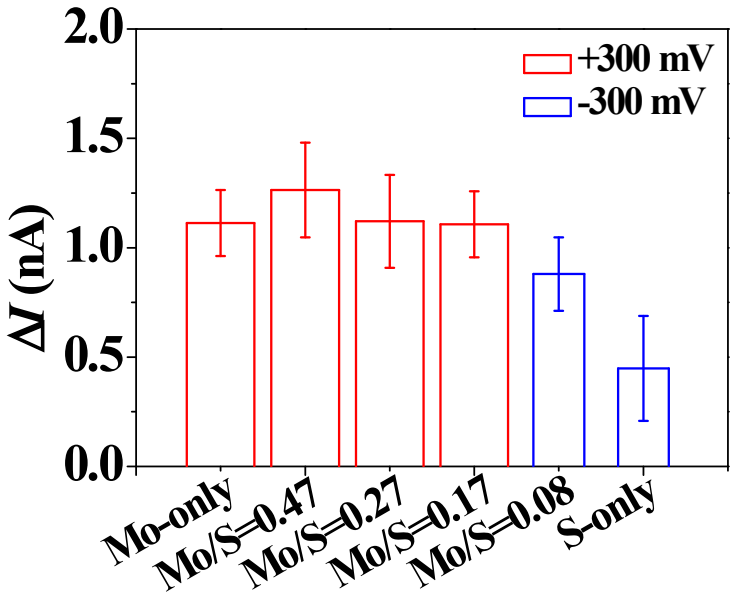

Figure S1. The average current blockades induced by ssDNA transport though nanopores with different proportion of Mo atoms to S atoms at the nanopore boundary. For each nanopore, the current blockade was averaged over the current blockades obtained from five independent simulations. Error bars represent the standard errors.

Method: Calculations of the local density of MoS_2 and local flux of ions.

The calculations of local densities of MoS_2 and the fluxes of ions were performed on a 50 × 50 × 76 cubic grid using the method described by Göpfrich, et al.[1] and Li, et al.[2]. The change in the coordinates (r) of the ion i between consecutive frames is $\Delta r_i(t+\Delta t/2) = (\Delta x_i(t+\Delta t/2), \Delta y_i(t+\Delta t/2), \Delta z_i(t+\Delta t/2))$, where Δt is the time interval between the two consecutive frames of the trajectory. To compute local fluxes, a regular orthogonal N_x*N_y*N_z grid was used to divide the simulation box into N_x*N_y*N_z rectangular blocks with identical dimensions $l_x=L_x/N_x$, $l_y=L_y/N_y$ and $l_z=L_z/N_z$ (where L_x, L_y and L_z are the side lengths of the box). A set of indices (l,m,n) indicates the position of each block in x, y and z directions. To compute the contribution of displacement vector of ion i, $\Delta r_i(t+\Delta t)$, to the local flux through each block, the ion was assumed to move from $r_i(t)$ to $r_i(t+\Delta t)$ along a straight line. Then, the fraction of the displacement vector in each of the $N_xN_yN_z$ blocks was determined, $f_{i,(l,m,n)}(t+\Delta t)$ such that $\sum_l \sum_m \sum_n f_{i,(l,m,n)}(t+\Delta t/2) = 1$. Finally, we defined the components of the instantaneous local flux per unit area of a chosen species in block (l,m,n) as

$$\phi_{x,(l,m,n)}(t+\Delta t/2) = \frac{1}{\Delta t l_x l_y l_z} \sum_i^{N_0} \Delta x_i(t+\Delta t/2) f_{i,(l,m,n)}(t+\Delta t/2)$$

$$\phi_{y,(l,m,n)}(t+\Delta t/2) = \frac{1}{\Delta t l_x l_y l_z} \sum_i^{N_0} \Delta y_i(t+\Delta t/2) f_{i,(l,m,n)}(t+\Delta t/2)$$

$$\phi_{z,(l,m,n)}(t+\Delta t/2) = \frac{1}{\Delta t l_x l_y l_z} \sum_i^{N_0} \Delta z_i(t+\Delta t/2) f_{i,(l,m,n)}(t+\Delta t/2)$$

where N_0 is the total number of ions of a given species. By averaging the equations above over the production MD trajectories, the mean local flux vector field was calculated. And we also averaged the 3D vector filed over the y axis to visualize the mean 3D flux field using a 2D plot. By using the streamplot function of the matplotlib

library, the resulting 2D vector field was converted to streamline plots. The method is put in our supplementary information and we also make it clear in the caption of Figure 3a that how we calculate the local densities of MoS_2 and the flux of ions. Details of the highlighting and track changes could be seen in the caption of Figure 3 and the supplementary information of the revised manuscript.

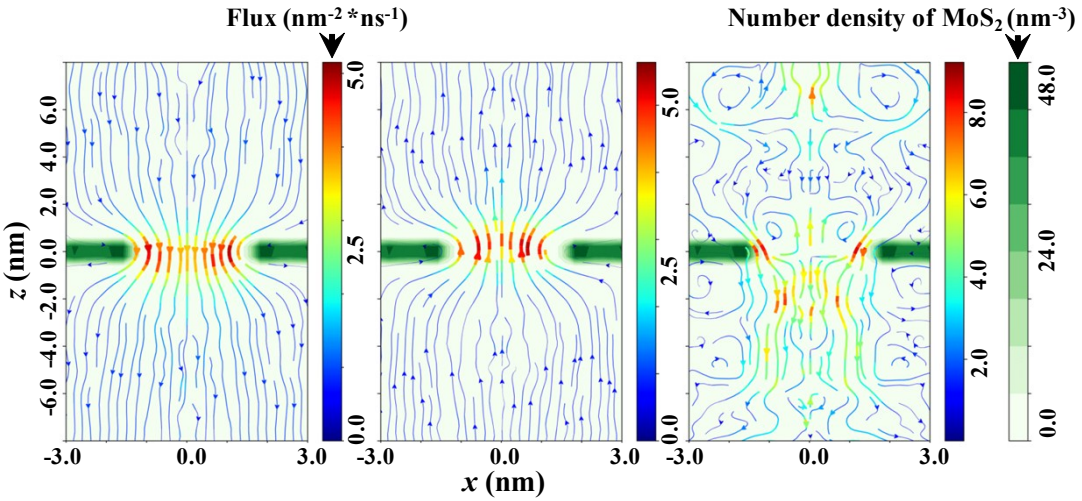

Figure S2. The 2D illustration of Cl^- flux (left), K^+ flux (middle) and water flux (right) through the nanopore with only Mo atoms at the nanopore boundary. A +300 mV was applied across the nanopore.

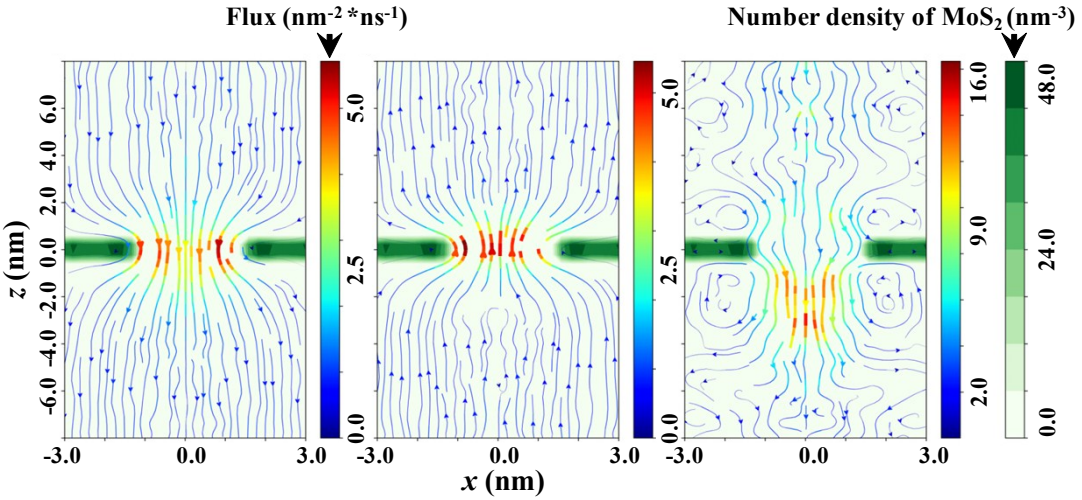

Figure S3. The 2D illustration of Cl^- flux (left), K^+ flux (middle) and water flux (right) through the nanopore with Mo/S equal to 0.47 at the nanopore boundary. A +300 mV was applied across the nanopore.

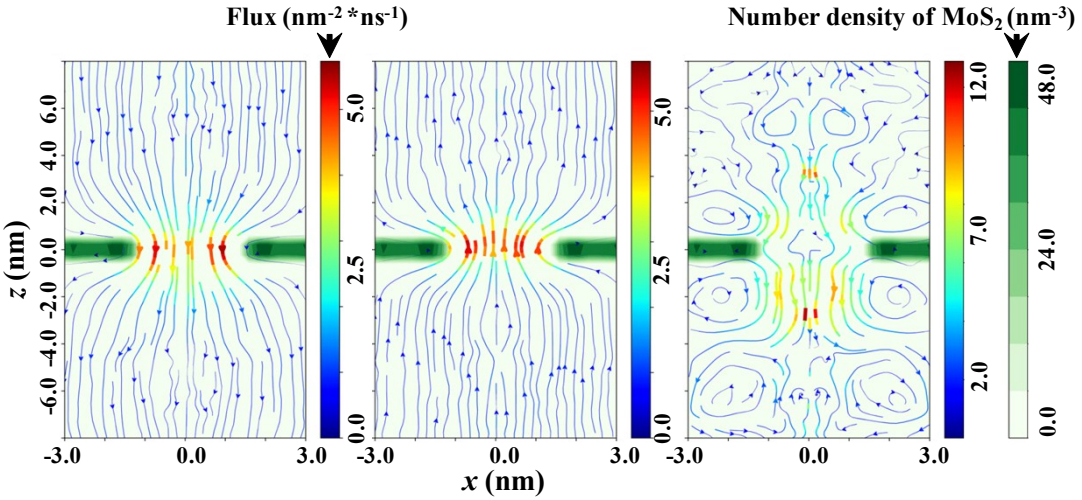

Figure S4. The 2D illustration of Cl^- flux (left), K^+ flux (middle) and water flux (right) through the nanopore with Mo/S equal to 0.27 at the nanopore boundary. A +300 mV was applied across the nanopore.

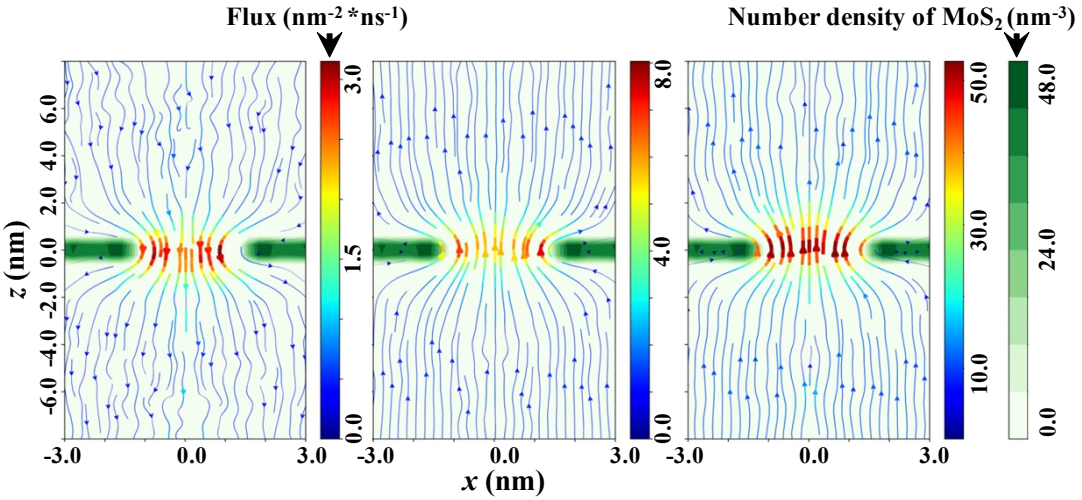

Figure S5. The 2D illustration of Cl^- flux (left), K^+ flux (middle) and water flux (right) through the nanopore with Mo/S equal to 0.08 at the nanopore boundary. A +300 mV was applied across the nanopore.

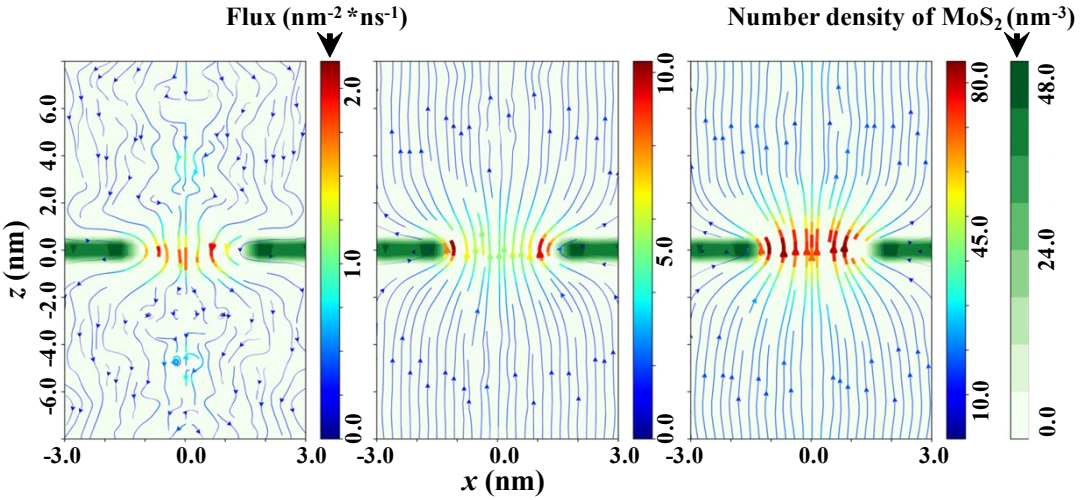

Figure S6. The 2D illustration of Cl^- flux (left), K^+ flux (middle) and water flux (right) through the nanopore with only S atoms at the nanopore boundary. A +300 mV was applied across the nanopore.

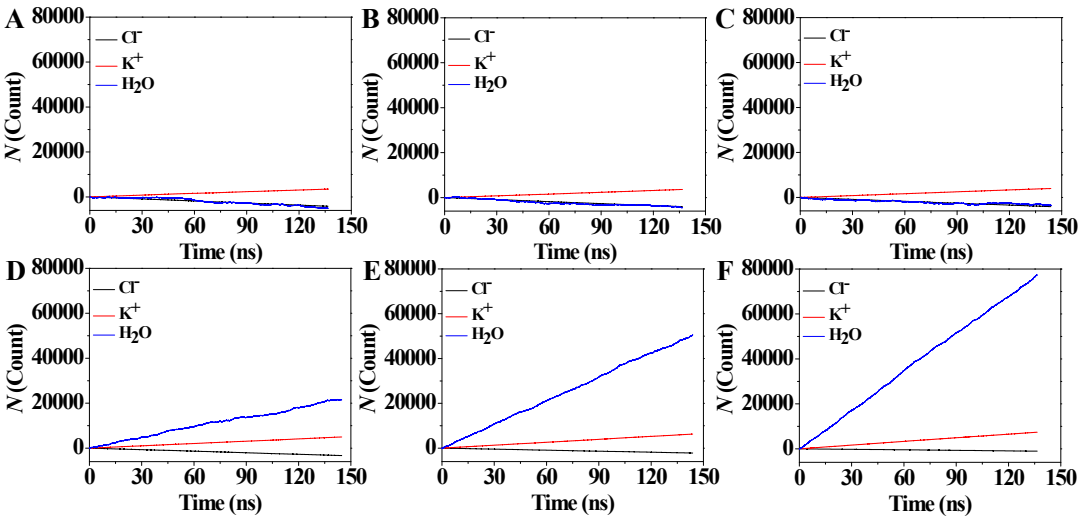

Figure S7. The integrated number of permeated ions and water molecules through the nanopores with only Mo atoms (A), Mo/S equal to 0.47 (B), 0.27 (C), 0.17 (D), 0.08 (E) and only S atoms (F) at the nanopore boundary. Positive (or negative) values indicate that the ions or water molecules moves in the same (or opposite) direction as the applied electric field. A +300 mV were applied across the nanopores.

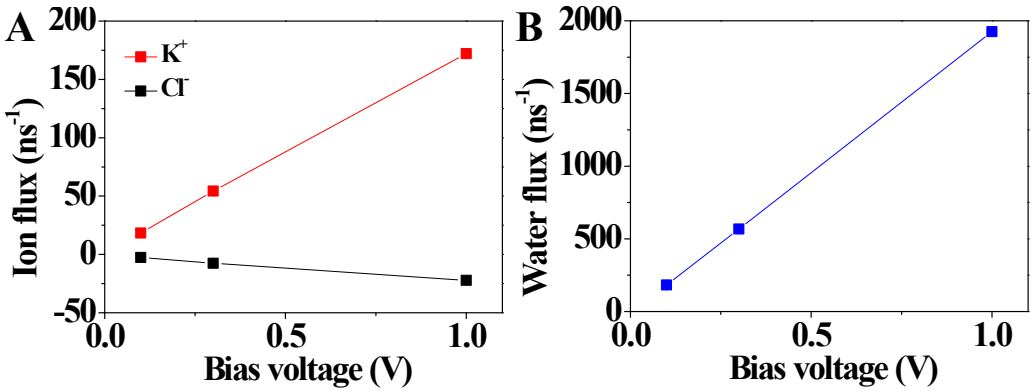

Figure S8. Amplitude of the ion flux (panel A) and water flux (panel B) through the 3 nm MoS_2 nanopore with only S atoms at the nanopore boundary.

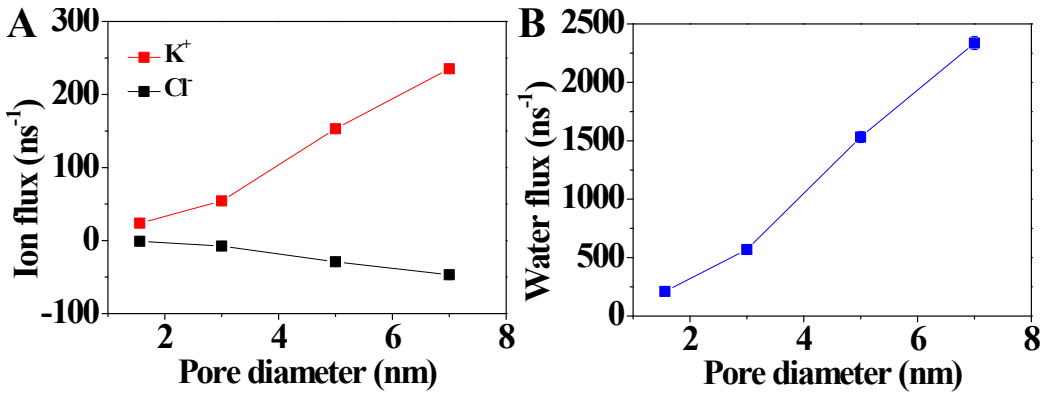

Figure S9. Amplitude of the ion flux (panel A) and water flux (panel B) through different diameter MoS_2 nanopores with only S atoms at the nanopore boundary. A +300 mV bias voltage was applied across the nanopores.

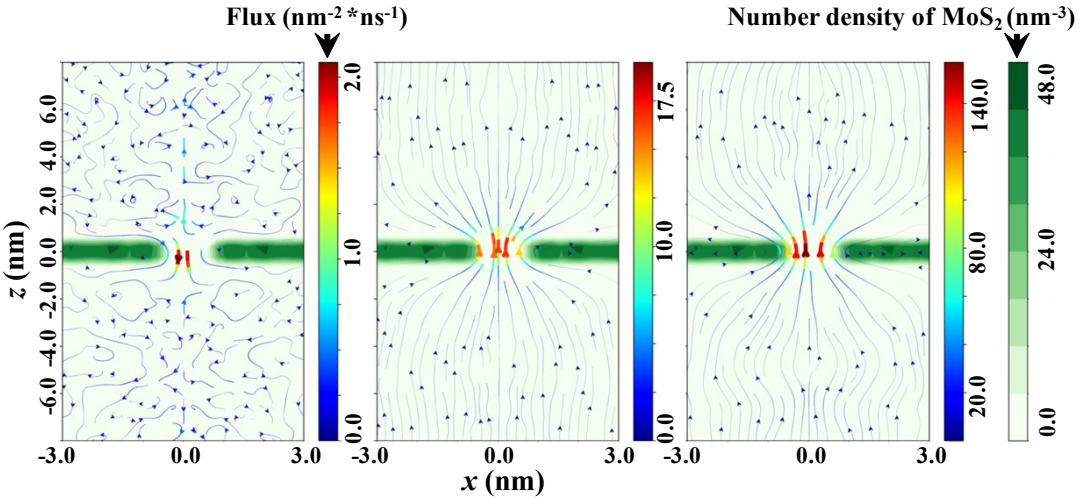

Figure S10. The 2D illustration of Cl^- flux (left), K^+ flux (middle) and water flux (right) through the 1.56 nm MoS_2 nanopore with only S atoms at the nanopore boundary. A +300 mV was applied across the nanopore.

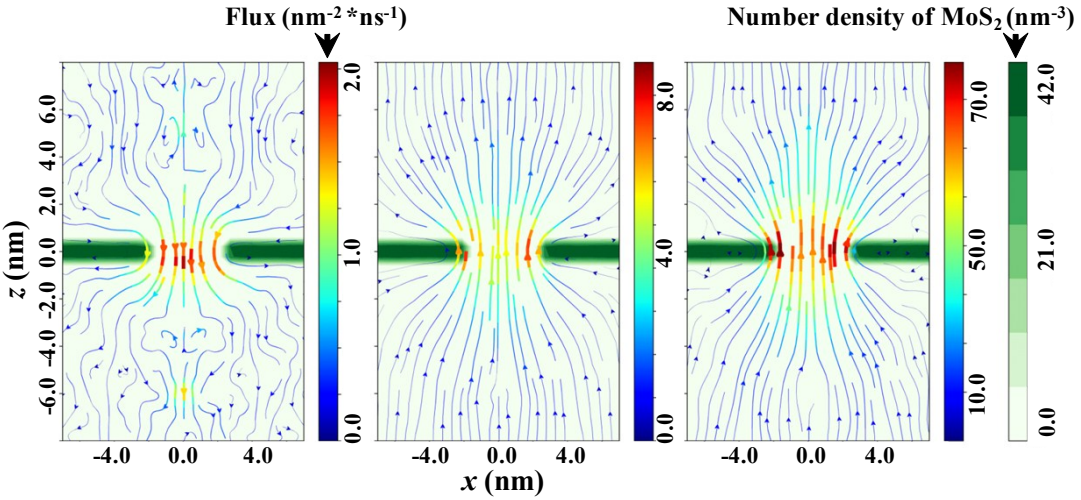

Figure S11. The 2D illustration of Cl^- flux (left), K^+ flux (middle) and water flux (right) through the 5 nm MoS_2 nanopore with only S atoms at the nanopore boundary. A +300 mV was applied across the nanopore.

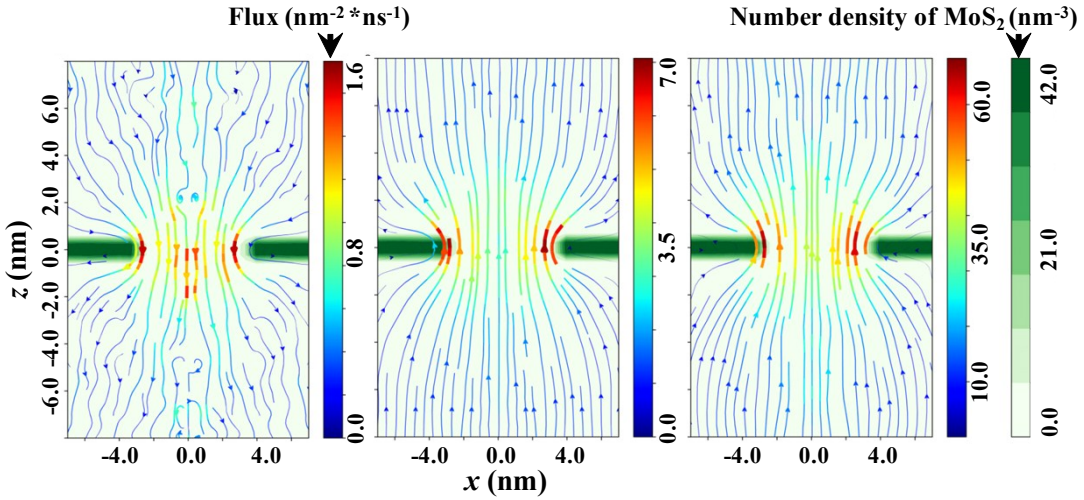

Figure S12. The 2D illustration of Cl^- flux (left), K^+ flux (middle) and water flux (right) through the 7 nm MoS_2 nanopore with only S atoms at the nanopore boundary. A +300 mV was applied across the nanopore.

1. K. Göpfrich, C.-Y. Li, M. Ricci, S. P. Bhamidimarri, J. Yoo, B. Gyenes, A. Ohmann, M. Winterhalter, A. Aksimentiev and U. F. Keyser, *Acs Nano*, 2016, **10**, 8207-8214.
2. C. Y. Li, E. A. Hemmig, J. Kong, J. Yoo, S. Hernandez-Ainsa, U. F. Keyser and A. Aksimentiev, *Acs Nano*, 2015, **9**, 1420-1433.